# Boron isotopes reveal multiple metasomatic events in the mantle beneath the eastern North China Craton

Hong-Yan Li [a,*], Zhou Zhou [a,b], Jeffrey G. Ryan [c], Gang-Jian Wei [a], Yi-Gang Xu [a]

[a] *State Key Laboratory of Isotope Geochemistry, Guangzhou Institute of Geochemistry, Chinese Academy of Sciences, Guangzhou 510640, China*
[b] *University of Chinese Academy of Sciences, Beijing 100049, China*
[c] *School of Geosciences, University of South Florida, Tampa, FL 33620, United States*

## Abstract

Linkages inferred between the geochemical heterogeneity of the mantle beneath eastern Eurasia and the stagnant Pacific slab documented geophysically in its mantle transition zone are as yet not clearly characterized. In this paper we report new elemental and isotopic data for boron (B) on a suite of well-characterized Cenozoic basalts (alkali basalts, basanites and nephelinites), with ocean island basalt (OIB)-like trace element signatures from western Shandong of the eastern North China Craton (NCC). Correlations between major elements (e.g., $FeO^T$ versus $SiO_2$), trace elements (e.g., $Ce_N/Pb_N$ versus $Ba_N/Th_N$) and radiogenic isotopes (e.g., $^{206}Pb/^{204}Pb$ versus $^{87}Sr/^{86}Sr$) suggest these basalts are derived via the mixing of melts from two mantle components: a fluid mobile element (FME; such as Ba, K, Pb and Sr) enriched component, which is most evident in the alkali basalts, and a FME depleted mantle component that is more evident in the basanites and nephelinites. The alkali basalts in this study have lower B concentrations (1.4–2.2 μg/g) but higher $\delta^{11}B$ (−4.9 to −1.4) values than the basanites and nephelinites (B = 2.1–5.0 μg/g; $\delta^{11}B$ = −6.9 to −3.9), and all the samples have nearly constant B/Nb ratios between 0.03 and 0.07, similar to the observed range in B/Nb for intraplate lavas. Our high-$SiO_2$ samples have higher $\delta^{11}B$ than that of our low $SiO_2$ samples, indicating that the B isotopic differences among our samples do not result from the addition of a continental crustal component in the mantle source, or direct crustal assimilation during the eruption process. The positive B versus Nb correlation suggests the B isotopic compositions of the western Shandong basalts primarily reflect the pre-eruptive compositions of their mantle sources. Correlations among B, Nd and Sr isotope signatures of the western Shandong basalts differ from those among basalts from plume settings (e.g., Azores and Hawaii), and are inconsistent with models suggesting single-step metasomatic additions to the mantle. We thus call upon multiple metasomatic events in the mantle beneath the eastern NCC in order to interpret its observed radiogenic and boron isotopic variability. The heavier $\delta^{11}B$, FME-enriched mantle source developed during an older event, while metasomatism by melts from the stagnant Pacific plate in the MTZ led to the development of a FME-depleted mantle source at greater depths with a lower $\delta^{11}B$.
© 2016 Elsevier Ltd. All rights reserved.

*Keywords:* Boron isotope; North China Craton; Intracontinental basalts; Recycled oceanic crust

## 1. INTRODUCTION

Subduction of oceanic crust plays the key role on recycling of earth-surface materials into the mantle (e.g., Plank and Langmuir, 1998; Sleep and Zahnle, 2001). Recent geophysical and geochemical findings indicate that subducted oceanic crust is likely responsible for

* Corresponding author. Fax: +86 20 85291510.
*E-mail address:* hongyanli@gig.ac.cn (H.-Y. Li).

heterogeneity in the mantle in intracontinental settings as well as in sub-arc settings (e.g. Pearce et al., 2007; Faccenna et al., 2010; Schmandt et al., 2014; Thomson et al., 2016). The high $H_2O$ storage capacity (1–3% wt.) of the high-pressure phases wadsleyite and ringwoodite present the possibility that the mantle transition zone (MTZ, 410–660 km) could host a large reservoir for $H_2O$ in the deep earth (Huang et al., 2005; Pearson et al., 2014). Seismic experimental and field investigations suggest the MTZ may act as a filter for fluids from the subducted oceanic slab (e.g., Bercovici and Karato, 2003; Schmandt et al., 2014). In addition, melting experiments on carbonated mid ocean ridge basalts (MORBs) suggest that a majority of subducted oceanic crust geotherms are likely to intersect their solidi at depths of approximately 300–700 km (Thomson et al., 2016). Therefore, dehydration or decarbonation melting of the subducted oceanic slab in or near the MTZ has the ability to refertilize the overlying mantle and reduce its solidus, with the potential to trigger mantle melting at shallower depths (Dasgupta et al., 2007, 2009; Faccenna et al., 2010; Wang et al., 2015). However, the question of how subducted oceanic slabs might affect the heterogeneity of the mantle in an intracontinental setting, or foster its partial melting, is unclear.

A stagnant subducted segment of the Pacific plate, identifiable via its high seismic velocities, has been imaged via P-wave tomography in the MTZ beneath eastern Eurasia (e.g., Fukao et al., 1992; Zhao, 2004; Zhao et al., 2009). In eastern China, Cenozoic intracontinental basalts occur primarily along its eastern continental margin, and their pattern of geographic distribution appears to be associated with that of the stagnant Pacific slab in the MTZ (Fig. 1a; Xu et al., 2012a; Li et al., 2016). These observations suggest that eastern Eurasia is a potentially ideal place to study relationships between mantle heterogeneity, magama generation and materials released from deeply subducted oceanic plates (e.g. Zhao et al., 2009; Kuritani et al., 2011; Tang et al., 2014; Wang et al., 2015).

There are three competing models supporting or challenging the notion that the stagnant Pacific slab in the MTZ has contributed enriched components to the sources of Cenozoic basalts in eastern China. The first model advocates wet upwelling triggered by dehydration of the stagnant Pacific slab in the MTZ (i.e., the MTZ acting as one mantle reservoir comprising materials from different subduction episodes), induced intracontinental magmatism in eastern China (e.g., Zhao et al., 2009; Kuritani et al., 2011; Wang et al., 2015; Guo et al., 2016). In this model, the enriched components in these Cenozoic basalts are from the MTZ. A second model suggests that contributions from the subducted Pacific slab are related to melting of carbonated oceanic crust (Sakuyama et al., 2013; Li et al., 2016), and also emphasizes the contribution of pre-existing enriched "plums" in the asthenospheric mantle (Li et al., 2016). The third competing model argues against a role of subducted Pacific slab materials in the MTZ in the generation of Cenozoic basalts in eastern China, postulating instead that the enriched component in these basalts arises from delaminated lower continental crust of the eastern
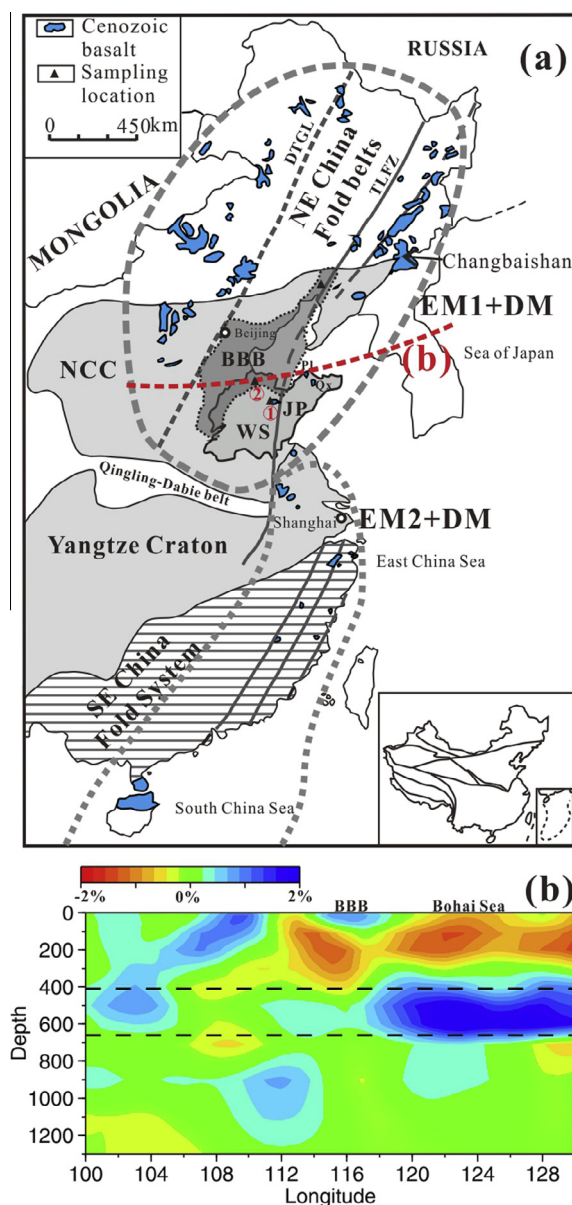


Fig. 1. (a) Simplified geological map of the eastern China with distributions of Cenozoic basalts and their mantle components (modified after Li et al., 2016). Sample locations are marked in black triangles: ① Changwei depression; ② Dashan of Wudi. NCC: North China Craton; BBB: Bohai Bay Basin; WS: Western Shandong; JP: Jiaodong Peninsula; DTGL: Daxinganling–Taihang Gravity Lineament; TLFZ: Tan-Lu Fault Zone; Pl: Penglai; Qx: Qixia. (b) Vertical cross section of P wave velocity perturbations along the profile shown in the geological map (modified after Huang and Zhao, 2006).

North China Craton (NCC; e.g., Liu et al., 2008; Chen et al., 2009; Zeng et al., 2011).

This paper reports new elemental and isotopic data for the strongly fluid mobile trace element (FME) boron (B) in a suite of Miocene-Quaternary basalts from western Shandong of the eastern NCC. In combination with published geochemical data on these rocks, we place new

constraints on metasomatic events in the subcontinental mantle of eastern China. Boron (B) isotopes [reported as $\delta^{11}B = (({}^{11}B/{}^{10}B)_{sample}/({}^{11}B/{}^{10}B)_{NBS\ 951} - 1) * 1000$] can provide valuable information on mantle heterogeneity (Chaussidon and Jambon, 1994; Tanaka and Nakamura, 2005; Turner et al., 2007) as: (a) B is extremely fluid mobile and is present in low concentrations in the mantle ($\sim$0.05–0.10 $\mu$g/g) at low $\delta^{11}B$ values ($-4.0 \pm 1.6‰$ to $-9.9 \pm 1.3‰$; Chaussidon and Jambon, 1994; Chaussidon and Marty, 1995; LeRoux et al., 2004; Turner et al., 2007); and (b) there are clear contrasts among the B isotope signatures of fresh oceanic crust, altered oceanic crust, marine sediments and continental crust (Ishikawa and Nakamura, 1992; Smith et al., 1995; Spivack and Edmond, 1987; Kasemann et al., 2000; van Hinsberg et al., 2011; Marschall and Jiang, 2011), which may relate to possible enriched components in the mantle of eastern China.

## 2. GEOCHEMICAL BACKGROUND AND SAMPLES

Cenozoic intraplate basalts are largely concentrated along two belts in eastern China: the Daxinganlin–Taihang gravity lineament (DTGL) and the Tan-Lu fault zone (Fig. 1a; Zhou and Armstrong, 1982; Fan and Hooper, 1991; Xu et al., 2012a). The lavas are primarily tholeiites, alkali basalts, trachybasalts, basanites, and nephelinites, e.g., basalts, erupted in Shandong province of eastern China (Zeng et al., 2010, 2011; Xu et al., 2012b; Li et al., 2014) and in the Changbaishan region in northeastern China (e.g., Kuritani et al., 2011; Fig. 1a). All these basalts show OIB-like trace element signatures, i.e. the enrichment of highly incompatible elements, enrichment of light rare earth elements (LREE) over heavy rare earth elements (HREE), and positive Nb-Ta anomalies on primitive mantle-normalized trace element variation plots (e.g., Zeng et al., 2010, 2011; Li et al., 2014, 2016; Kuritani et al., 2011).

The NCC, located in the central part of eastern China, is one of the world's oldest cratons ($\sim$3.8 Ga; Liu et al., 1992). The NCC is considered to be an amalgamation of the eastern and western blocks along the Trans-North China Orogen (approximately along the DTGL) during the Early Paleoproterozoic (ca. 1.85 Ga; Zhao et al., 2001). It is well documented that a >100 km thick lithospheric keel beneath the eastern NCC was removed during the Mesozoic and Cenozoic (Fan and Menzies, 1992; Griffin et al., 1992, 1998; Menzies et al., 1993; Zheng et al., 1998; Xu, 2001; Gao et al., 2004; Xu et al., 2004). Delamination of thickened continental lower crust has long been proposed as a cause for lithospheric thinning beneath the eastern NCC, based on radiogenic isotope studies (e.g., Gao et al., 2004; Wu et al., 2005; Liu et al., 2008). Therefore, the petrogenesis of Cenozoic basalts in the eastern NCC has significance in both testing the mechanisms for lithospheric thinning beneath the eastern NCC and for examining the geochemical evolution of the mantle in response to materials released from the subducted Pacific slab in the MTZ.

This study focuses on the boron abundance and B isotope compositions of Miocene alkali basalts and basanites from the Changwei depression, and Quaternary nephelinites from Dashan of Wudi in the western Shandong region of the eastern NCC (Fig. 1a). The bulk rock major element, trace element and radiogenic Sr-Nd-Hf-Pb isotopes (Fig. 2; Supplemental Figures) for these basalts have been discussed in detail by Zeng et al. (2010, 2011), Xu et al. (2012b), Sakuyama et al. (2013) and Li et al. (2016). All of the samples have minor olivine and clinopyroxene phenocrysts in a groundmass of olivine, plagioclase, clinopyroxene, Ti-magnetite, and glass. The olivines are very fresh, and almost all lack iddingsite rims, indicating that their eruptive B isotopic signatures should be well preserved (Tanaka and Nakamura, 2005).

The higher $SiO_2$ samples of this study are less alkaline, and show lower CaO, $FeO^T$, and incompatible element concentrations, as well as lower La/Yb and Sm/Yb, lower $Ce_N/Pb_N$ ratios and higher $Ba_N/Th_N$ ratios and $Sr^*/Sr$ anomalies [Fig. 2a, b and Supplemental Figures; N: primitive mantle (McDonough and Sun, 1995) normalized; $Sr^*/Sr = 2 \times Sr_N/(Pr_N + Nd_N)$]. Isotopically, the higher $SiO_2$ basalts have less radiogenic ${}^{176}Hf/{}^{177}Hf$, ${}^{143}Nd/{}^{144}Nd$ and ${}^{206}Pb/{}^{204}Pb$ but more radiogenic ${}^{87}Sr/{}^{86}Sr$ than do the lower $SiO_2$ samples, suggesting a greater contribution from an EMI-like mantle source (Fig. 2c and Supplemental Figures). In Hf-Nd isotope space, the higher $SiO_2$ basalts fall in the Indian mantle domain while the nephilinites fall in the Pacific mantle domain (Supplemental Figures).

The western Shandong basalts have a wide range of $\varepsilon_{Nd}(t)$ values from $-1.3$ to $+6.0$. However, they have nearly constant Th/Nb ratios, between 0.06 and 0.09 (Table 1), which are much lower than the value for bulk continental crust (Th/Nb = 0.70, Rudnick and Gao, 2003) but are similar to OIBs (Th/Nb = 0.08, Sun and McDonough, 1989). These features rule out crustal contamination as producing significant compositional variations within the western Shandong basalts (Li et al., 2016). The western Shandong basalts span a relatively narrow range of $Mg^\#$ [defined as $Mg^\# = 100 \times Mg/(Mg + 0.85 \times Fe^{total})$, where Mg and Fe are molar concentrations], from 60 to 69, with the nephelinites have systematically lower $SiO_2$ and $Al_2O_3$, but higher MgO, $FeO^T$ and CaO than the basanites and alkali basalts (Supplemental Table 1). This suggests that while these basalts have undergone only limited extents of fractional crystallization, mixing of melts played the key role in their chemical characteristics.

The higher $SiO_2$ basalts of this study show EMI-like isotopic and trace element signatures (e.g., positive Ba anomalies on normalized spider diagrams), but are richer in K, Pb and Sr than the Gough and Tristan da Cunha basalts that typify the EMI mantle source (Willbold and Stracke, 2006; Fig. 2a). The enriched EMI signature in these higher $SiO_2$ basalts is inferred to derive from garnet pyroxenite domains within their mantle source (Zeng et al., 2010; Xu et al., 2012b; Li et al., 2016). Interestingly, the associated nephelinites show high-$\mu$ (HIMU; high ${}^{238}U/{}^{204}Pb$) type trace element characteristics (i.e., depletion of Rb-Ba relative to Nb and negative K-Pb anomalies on mantle-normalized spidergrams; Willbold and Stracke, 2006; Fig. 2a). Data for magmatic olivines and associated melt inclusions suggest a mixed and carbonated peridotite-garnet pyroxenite mantle

source for the nephelinites (Li et al., 2016). In this study, we use the terms FME-rich and FME-depleted mantle sources (fluid-mobile elements: FME, defined here as Ba, K, Pb, Sr, and B) to distinguish among the high and low $SiO_2$ basalts, respectively.

The western Shandong basalts fall on mixing trends in terms of major elements (e.g., $FeO^T$ versus $SiO_2$; Supplemental Figures), trace elements (e.g., $Ce_N/Pb_N$ versus $Ba_N/Th_N$; Fig. 2b) and radiogenic isotopes (e.g., $^{206}Pb/^{204}Pb$ versus $^{87}Sr/^{86}Sr$; Fig. 2c) suggesting the mixing
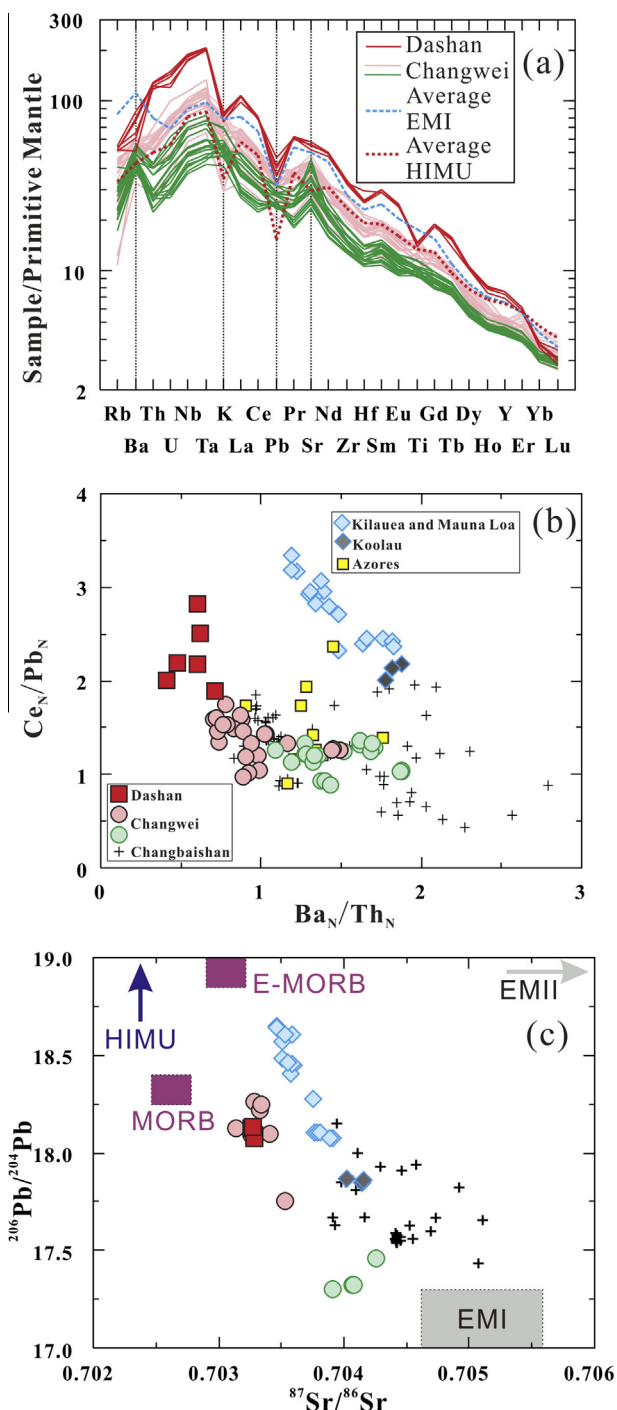
of melts from different mantle sources (Zeng et al., 2010, 2011; Xu et al., 2012b; Sakuyama et al., 2013; Li et al., 2016). The EMI-like ($^{206}Pb/^{204}Pb$ approximately from 16.8 to 17.8; Zindler and Hart, 1986) component, which is prominent in the FME-rich mantle source, requires old (>1.0 Ga) low-μ ($^{238}U/^{204}Pb$) materials to develop its low $^{206}Pb/^{204}Pb$ isotopic signature (Rehkämper and Hofmann, 1997; Murphy et al., 2003). This signature cannot be derived from recently subducted Pacific slab (Kuritani et al., 2011). Hf-Nd isotopic modeling of the origins for this FME rich mantle source leads to two possibilities: that this mantle source includes contributions from ancient marine sediments and oceanic crust (Supplemental Figures; Li et al., 2014; Liu et al., 2015), or that delaminated and evolved lower continental crust is responsible for its signature (e.g., Chen et al., 2009; Zeng et al., 2010). By contrast, the FME-depleted mantle source has HIMU-like trace element signatures but MORB-like Sr-Pb isotopic systematics (Fig. 2a, c), indicating it includes inputs from young subducted oceanic crust (Xu et al., 2012a; Sakuyama et al., 2013). This is consistent with published conclusions that the nephelinites carry the Hf–Nd isotopic fingerprint of Pacific Ocean crust (Supplemental Figures; Sakuyama et al., 2013; Li et al., 2016).

Kuritani et al. (2011) have proposed a two-stage model to explain the apparent mantle heterogeneity beneath northeast China. First, an ancient (>1.0 Ga ago) slab dehydration event metasomatized the MTZ with fluids from subducted sediments. Dehydration of the recently subducted Pacific slab refertilized the MTZ by injecting a more recent enriched component, and triggered wet upwelling of the MTZ that facilitated the transit of enriched materials (both ancient and more recent) to shallower mantle depths, where these materials were sampled during magmatism in the Changbaishan area (Fig. 1a). Because the FME-depleted basalts have HIMU-like trace element signatures but less radiogenic $^{206}Pb/^{204}Pb$ than typical HIMU sources



Fig. 2. (a) Primitive mantle (McDonough and Sun, 1995) normalized trace element patterns, (b) $Ce_N/Pb_N$-$Ba_N/Th_N$ correlations (data from Zeng et al., 2010, 2011; Li et al., 2016), and (c) $^{206}Pb/^{204}Pb$ versus $^{87}Sr/^{86}Sr$ correlations for western Shandong basalts (data from Xu et al., 2012b; Sakuyama et al., 2013). In (a), the average EMI is according the average data of Gough and Tristan da Cunha basalts, while the average HIMU is according the average data of St. Helena basalts (Willbold and Stracke, 2006). In (b), the Ce, Pb, Ba and Th are primitive mantle normalized according McDonough and Sun (1995). In (c), the fields of average mid-ocean ridge basalts (MORB) and enriched mid-ocean ridge basalts (E-MORB) are according Su and Langmuir (2003) and Workman and Hart (2005), respectively. The field of enriched mantle I (EMI) is according Zindler and Hart (1986). In (b) and (c), the data of the Changbaishan region basalts are also plotted in the context. It include samples with >7% MgO from Changbaishan, Zengfengshan, Longgang, Wanqing, Jingbohu, Mudanjiang and Kuandian (Basu et al., 1991; Liu et al., 1994; Hsu et al., 2000; Chen et al., 2003, 2007; Zou et al., 2008; Yan and Zhao, 2008; Kuritani et al., 2009, 2011). The data of Kilauea, Mauna Loa and Koolau of Hawaiian chain are from Tanaka et al. (2002) and Tanaka and Nakamura (2005), the data of Azores are from Turner et al. (1997).

Table 1
B elemental and isotopic composition and selected elemental and Sr-Nd isotope data of the western Shandong basalts.

| Sample | SiO$_2$ (wt%) | TiO$_2$ (wt%) | MgO (wt%) | FeO$^T$ (wt%) | Mg$^{\#}$ | Nb (µg/g) | Th/Nb | K/Rb | La/Yb | Sm/Yb | Ce$_N$/Pb$_N$ | Ba$_N$/Th$_N$ | Sr/Sr$^*$ | $^{87}$Sr/$^{86}$Sr | $\varepsilon_{Nd}$ | B (µg/g) | $\delta^{11}$B | SE |
|---|---|---|---|---|---|---|---|---|---|---|---|---|---|---|---|---|---|---|
| 07CDS05 | 47.08 | 1.85 | 9.51 | 10.52 | 65.5 | 30.8 | 0.07 | 1047 | 16.9 | 3.7 | 1.3 | 1.7 | 1.4 | 0.703687 | −0.5 | 1.5 | −3.61 | 0.05 |
| 07CDS06 | 47.10 | 1.86 | 9.37 | 10.46 | 65.2 | 30.8 | 0.07 | 1057 | 16.7 | 3.7 | 1.2 | 1.7 | 1.4 | 0.703695 | −0.7 | 1.4 | −1.38 | 0.05 |
| 07CDS07 | 47.64 | 1.90 | 8.56 | 10.37 | 63.4 | 32.3 | 0.07 | 1001 | 16.7 | 3.6 | 1.3 | 1.7 | 1.4 | 0.703782 | −0.9 | 1.5 | −2.48 | 0.04 |
| 07FS01 | 43.68 | 3.04 | 8.76 | 12.49 | 59.5 | 68.4 | 0.07 | 466 | 30.1 | 5.7 | 1.6 | 0.9 | 1.3 | 0.703290 | 5.2 | 3.3 | −5.45 | 0.03 |
| 07FS03 | 43.20 | 2.86 | 9.52 | 12.77 | 61.0 | 66.3 | 0.07 | 380 | 31.3 | 6.0 | 1.8 | 0.8 | 1.2 | 0.703297 | 4.9 | 3.0 | −6.30 | 0.03 |
| 07FYS02 | 47.62 | 2.00 | 8.18 | 10.48 | 62.1 | 29.0 | 0.06 | 864 | 14.4 | 3.5 | 1.0 | 1.9 | 1.4 | 0.704035 | −0.1 | 1.6 | | |
| 07FYS09 | 47.38 | 2.03 | 9.02 | 10.54 | 64.2 | 40.9 | 0.07 | 648 | 18.7 | 3.9 | 1.2 | 1.4 | 1.4 | 0.704459 | 1.7 | 1.4 | | |
| 07LIS02 | 46.93 | 2.11 | 8.69 | 11.27 | 61.8 | 45.7 | 0.07 | 1004 | 22.3 | 4.3 | 1.3 | 1.1 | 1.4 | 0.703613 | 2.6 | 2.2 | −3.34 | 0.04 |
| 07LIS04 | 47.46 | 2.11 | 8.08 | 11.44 | 59.7 | 45.9 | 0.07 | 1019 | 22.3 | 4.3 | 1.1 | 1.2 | 1.4 | 0.703633 | 2.7 | 2.0 | −4.87 | 0.04 |
| 07LS05 | 43.78 | 2.40 | 9.84 | 11.87 | 63.5 | 64.4 | 0.07 | 1010 | 33.3 | 5.8 | 1.3 | 0.7 | 1.2 | 0.703400 | 3.9 | 2.1 | −3.87 | 0.03 |
| 07SW01 | 47.42 | 1.98 | 10.04 | 11.27 | 65.1 | 25.7 | 0.09 | 760 | 12.9 | 3.2 | 0.9 | 1.4 | 1.3 | 0.704306 | 0.1 | 1.7 | −3.40 | 0.04 |
| 07SW03 | 47.44 | 1.89 | 10.64 | 11.18 | 66.6 | 24.5 | 0.09 | 710 | 12.6 | 3.2 | 0.9 | 1.4 | 1.4 | 0.704437 | −1.4 | 1.7 | | |
| 07THS02 | 43.60 | 2.68 | 11.54 | 11.38 | 68.0 | 59.2 | 0.07 | 687 | 21.4 | 4.2 | 1.4 | 1.0 | 1.3 | 0.703268 | 5.6 | 3.1 | −5.55 | 0.03 |
| 07THS03 | 43.67 | 2.68 | 11.09 | 11.39 | 67.1 | 60.5 | 0.07 | 674 | 21.5 | 4.1 | 1.4 | 1.0 | 1.3 | 0.703332 | 5.8 | 3.2 | −6.90 | 0.03 |
| WF12 | 43.51 | 2.72 | 10.30 | 11.27 | 65.7 | 56.8 | 0.08 | 680 | 23.4 | 4.2 | 1.2 | 1.0 | 1.1 | 0.703282 | 5.2 | 2.1 | −5.11 | 0.04 |
| WF22 | 43.98 | 2.71 | 10.42 | 11.26 | 66.0 | 60.1 | 0.08 | 740 | 22.6 | 3.9 | 1.3 | 0.9 | 1.1 | 0.703353 | 5.3 | 2.9 | −4.99 | 0.04 |
| WF32 | 44.08 | 2.79 | 10.82 | 11.18 | 67.0 | 63.5 | 0.08 | 709 | 21.9 | 4.0 | 1.0 | 0.9 | 1.1 | 0.703306 | 5.2 | 3.4 | −6.67 | 0.03 |
| | | | | | | | | | | | | | | | | | −6.67 | 0.05 |
| YS11 | 43.84 | 2.60 | 10.10 | 11.86 | 64.1 | 64.0 | 0.08 | 760 | 26.6 | 5.0 | 1.5 | 0.7 | 1.3 | 0.703918 | 5.1 | 3.3 | −4.84 | 0.03 |
| YS13 | 43.82 | 2.59 | 10.05 | 11.87 | 64.0 | 63.2 | 0.08 | 730 | 27.5 | 5.2 | 1.5 | 0.8 | 1.2 | 0.703688 | 5.1 | 3.1 | −6.24 | 0.03 |
| | | | | | | | | | | | | | | | | | −6.42 | 0.05 |
| CZ | 40.96 | 2.91 | 11.93 | 14.45 | 63.4 | 122.9 | 0.08 | 567 | 40.1 | 7.1 | 2.8 | 0.6 | 1.0 | 0.703611 | 5.9 | 5.0 | −5.01 | 0.03 |

Re-analysis of the same solution; N: primitive mantle (McDonough and Sun, 1995) normalized; Sr/Sr$^*$ = 2 × Sr$_N$/(Pr$_N$ + Nd$_N$); Mg$^{\#}$ = 100 × Mg/(Mg + 0.85 × Fe$^{total}$), where Mg and Fe are molar concentrations. The selected major element, trace element and Sr-Nd isotope data are from Zeng et al. (2010) and Li et al. (2016), the full data set is in Supplemental Table 1.

(Fig. 2c), a young (<1.0 Ga) ocean crustal component beneath east China is required (Xu et al., 2012a).

Ocean island basalts are conventionally attributed to decompression melting of deeply-derived hot mantle, driven by mantle plumes (e.g., Morgan, 1971). Although the mechanism is different, a wet upwelling model for intracontinental basalt generation in eastern China (Kuritani et al., 2011; Wang et al., 2015) has some similarity to the plume model for OIBs in that it mobilizes materials from a deeper mantle reservoir, i.e., the MTZ (Bercovici and Karato, 2003). Related to this, two different effects are possible as regards the B isotopic signatures in the MTZ: (1) As boron is strongly fluid-mobile and does not substitute well into any major silicate mineral phase in the mantle, B fluid-rock exchanges may serve to homogenize materials in the MTZ; or (2) The B isotopic signatures of materials in the MTZ preserve signatures related to their protoliths, i.e., either subducted sediment or crust. In either case, the basalts in the eastern NCC should reflect the mixing of MORB-source (with different degrees of alteration) materials and sediment-derived materials if they were generated via the wet upwelling model of Kuritani et al. (2011). The boron isotopes, given their sensitivity to subduction-related materials, should be capable of distinguishing among different enriched components in both FME-rich and depleted mantle sources, and among associated metasomatic phenomena.

## 3. ANALYTICAL METHODS

B abundance and B isotopic analyses were conducted in the State Key Laboratory of Isotope Geochemistry, Guangzhou Institute of Geochemistry, Chinese Academy of Sciences (GIGCAS). About 150 mg of rock powder was precisely weighed into a pre-cleaned 7 mL PFA-Teflon beaker, along with 100 μL 1% mannitol, 100 μL $H_2O_2$ and 1 mL 24 M HF. The beaker was tightly capped and placed on a hot plate at a temperature of 60 °C for 3 days for boron extraction. Both the solution and residue were then transferred into a pre-cleaned polypropylene (PP) tube, and centrifuged. The supernatant was collected, and boron was concentrated in this solution, at a recovery of >99% (Wei et al., 2013). The collected supernatant was then diluted with B-free Milli-Q deionized water to an HF molarity of 3 M for ion-exchange purification. The samples were loaded onto 20 ml columns with Bio-Rad AG MP-1 strong anion exchange resin for chromatographic purification, following procedures in Wei et al. (2013). The eluted boron was collected in a pre-cleaned 15 mL PFA beaker, and quantitatively diluted to 12 mL.

A 2 mL aliquot of this solution was taken for boron concentration measurement using a Varian Vista Pro inductively coupled plasma atomic emission spectrometer (ICP-AES) equipped with an HF-resistant Teflon spray chamber and an $Al_2O_3$ injector. Boron was measured using the 249.678 nm spectral line. Our column procedure separates Fe from B, so the large Fe spectral interference at 249.650 nm was minimized, which improved the effective detection limit to less than 0.01 μg/g B in solution, enabling measurement of boron concentrations at <1 μg/g in basalts.

Internal precision for our boron concentration determinations were generally better than 5% (RSD). Basalt standards B-5, JB-2 and JB-3 were measured multiple times as unknowns with our samples, yielding B concentrations of $10.17 \pm 0.22$ μg/g (1SD, $n = 3$), $29.98 \pm 0.98$ μg/g (1SD, $n = 4$) and $19.39 \pm 0.52$ μg/g (1SD, $n = 3$), respectively. Our results for B5 are consistent with the long-time monitoring value of 10.18 μg/g B in our laboratory.

The remaining 10 ml of our sample solutions were used for $\delta^{11}B$ measurement. 100 μL of 1% mannitol was added into each beaker to prevent volatilization losses of boron during drying. The 15 mL PFA beaker was then dried on a hot plate at temperature of 55 °C for 2–3 days. The dried samples were re-dissolved in 1.5 mL Milli-Q water, and then were further diluted to a boron concentration of $\sim 100$ ng mL$^{-1}$. $\delta^{11}B$ measurements were performed using a Finnegan Neptune MC-ICPMS in sample-standard-bracketing (SSB) mode. Details of the analytical procedures of $\delta^{11}B$ are described by Wei et al. (2013). The internal precision for $\delta^{11}B$ was better than $\pm 0.05‰$ (2σ standard error), and the external precision for $\delta^{11}B$ was better than $\pm 0.30‰$ (2 σ standard error) estimated by the long-term results of SRM 951 (Wei et al., 2013). Several basalt standards such as B5, JB-2 and JB-3 were repeatedly analyzed along with the samples, yielding the $\delta^{11}B$ results of $-4.78 \pm 0.30‰$ (1SD, $n = 3$), $7.16 \pm 0.31‰$ (1SD, $n = 4$) and $5.83 \pm 0.33‰$ (1SD, $n = 4$).

## 4. RESULTS

The B elemental and isotopic composition of the western Shandong basalts are presented in Table 1. While their fields show some overlap, the basanites have overall higher B concentrations (2.1–3.4 μg/g) than the alkaline basalts and trachy-basalts (B = 1.4–2.2 μg/g), while our one nephelinite, sample CZ, has the highest B concentration at 5.0 μg/g (Fig. 3a). The B concentrations of the western Shandong basalts correlate positively with their $TiO_2$ and Nb contents (Fig. 3b, c). All of the samples have B/Nb ratios between 0.03 and 0.07 (Fig. 4a), similar to the observed range in B/Nb for intraplate lavas reported by Ryan et al. (1996), Tanaka and Nakamura (2005) and Turner et al. (2007). Irrespective of overlap, the basanites and nephelinites have lower $\delta^{11}B$ ($-6.9‰$ to $-3.9‰$) than do the alkali basalts ($\delta^{11}B = -4.9‰$ to $-1.4‰$). $\delta^{11}B$ values of the western Shandong basalts are negatively correlated with their B concentrations (Fig. 4b).

## 5. DISCUSSION

### 5.1. Post-eruptive effects on B and B isotope systematics

The potential for post-eruptive effects, such as crustal assimilation, degassing and weathering, on the B elemental and isotopic composition of western Shandong basalts must be carefully evaluated, because these processes can easily modify an initial mantle-derived magmatic B composition (Spivack and Edmond, 1987; Chaussidon and Jambon, 1994; Genske et al., 2014). The continental crust preserves a low $\delta^{11}B$ value of $\sim -10‰$ (Kasemann et al.,
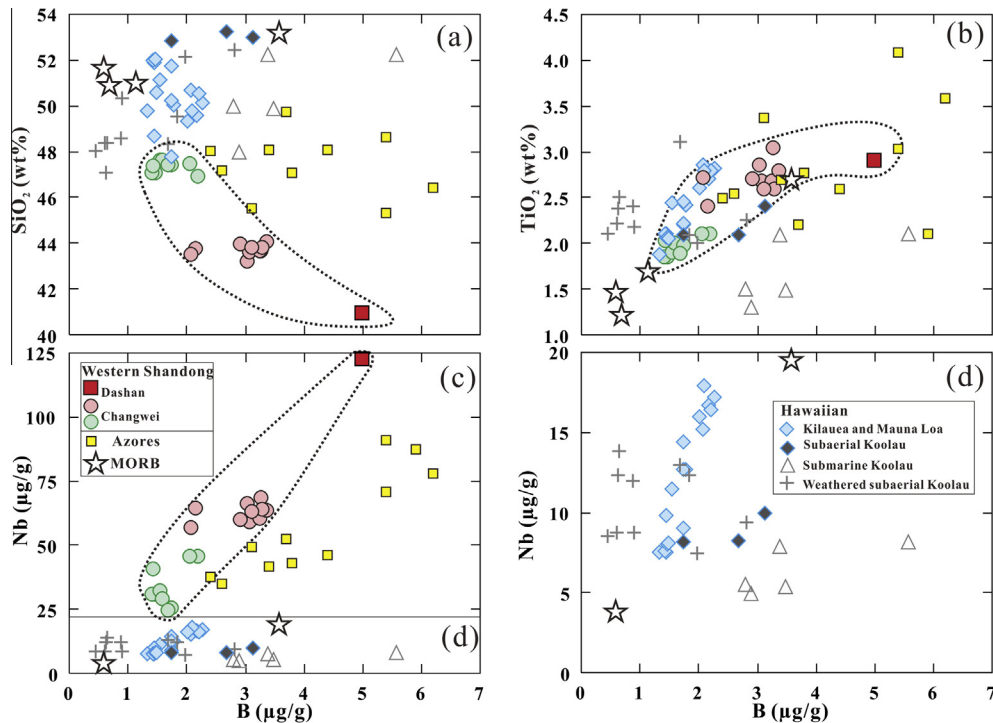
Fig. 3. $SiO_2$ (a), $TiO_2$ (b) and Nb (c, d) versus B diagrams for western Shandong basalts. The $SiO_2$, $TiO_2$, and Nb data of western Shandong basalts are from Zeng et al. (2010, 2011) and Li et al. (2016). The data source of Kilauea, Mauna Loa and Koolau of Hawaiian chain are from Tanaka et al. (2002) and Tanaka and Nakamura (2005), the data of Azores are from Turner et al. (1997, 2007), the data of MORB are from LeRoux et al. (2004).

2000; van Hinsberg et al., 2011; Marschall and Jiang, 2011). However, our high-$SiO_2$ samples have higher $\delta^{11}B$ than our low $SiO_2$ samples (Fig. 4), which indicates that the B isotopic differences among our samples are most likely not related to crustal assimilation. Nb and B are both strongly incompatible in mantle minerals, and appear not to be fractionated significantly during melting or crystallization (Ryan et al., 1996; Brenan et al., 1998a). Therefore, a positive correlation between B and Nb would be observed if the basalts preserve their pre-eruption B composition, like fresh basalts from Hawaii and the Azores (Fig. 3c, d; Tanaka and Nakamura, 2005; Turner et al., 2007; Genske et al., 2014). However, as B is strongly fluid-mobile (Ryan et al., 1996; Brenan et al., 1998a), a positive correlation between B and Nb will be destroyed if the B composition of basalts had suffered from any kind of post-eruptive effects, as was observed among weathered subaerial Koolau samples (e.g., Fig. 3d; Tanaka and Nakamura, 2005). The regular positive correlations between Nb, $TiO_2$ and B (Fig. 3b, c) suggest that the B concentrations of our western Shandong basalts are dominantly controlled by magmatic processes.

The fractionation of stable isotopes is controlled by reactivity differences among the isotopes. For both Li and B, the heavier isotopes (i.e., $^7Li$ and $^{11}B$) partition more readily into aqueous solution while the lighter isotopes (i.e., $^6Li$ and $^{10}B$) are better retained in minerals during low temperature weathering processes (Ishikawa and Nakamura, 1992; Hervig et al., 2002; Kısakűrek et al., 2005; Marschall et al., 2007). Low temperature weathering

also preferentially mobilizes Rb relative to K (Feigenson et al., 1983; Tanaka et al., 2002). Therefore, low temperature weathering of basalts (in the absence of seawater) after emplacement should reduce their B contents and $\delta^{11}B$ values but increase their K/Rb ratios (Tanaka and Nakamura, 2005). Based on the findings of Kuritani and Nakamura (2006), post-eruptive degassing can also decrease both B concentrations and $\delta^{11}B$ values, as vapor phases preferentially take up $^{11}B$ relative to coexisting melt and solid phases. Our alkali basalts and basanites show negative rather than positive correlations between B and $\delta^{11}B$ and a narrow range of K/Rb ratios, and there is no obvious correlation between K/Rb and $\delta^{11}B$ values (Fig. 4c, d). Thus, weathering or degassing are not major factors in the B elemental and isotopic composition of the Shandong basalts.

The observed boron abundance patterns are consistent with those of incompatible trace elements in the western Shandong during the Cenozoic. The B isotopic compositions of the western Shandong basalts primarily reflect the pre-eruptive compositions of their mantle sources, and the Nb/B and $\delta^{11}B$ are in the range of those observed in other intraplate settings (Tanaka and Nakamura, 2005; Turner et al., 2007; see also below).

### 5.2. The boron isotopic composition of the mantle

High-precision boron isotopic data for volcanic rocks derived from mantle sources away from subduction zones
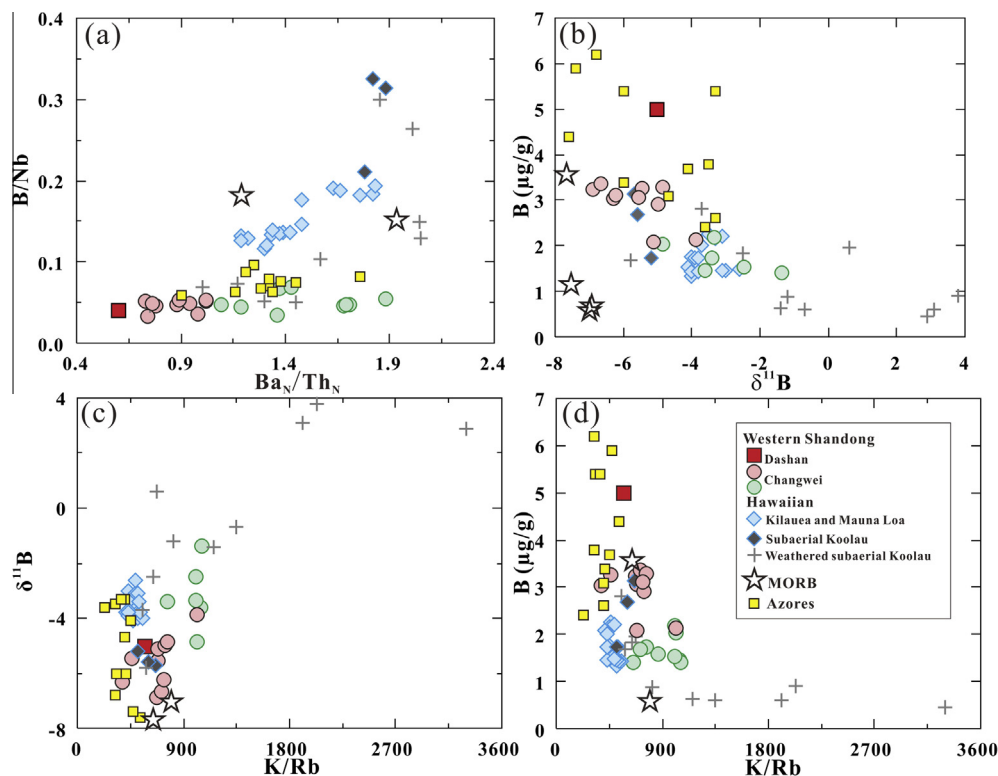
Fig. 4. B/Nb versus $Ba_N/Th_N$ (a), B versus $\delta^{11}B$ (b), $\delta^{11}B$ versus K/Rb (c) and B versus K/Rb (d) diagrams for western Shandong basalts. The Nb, K and Rb data are from Zeng et al. (2011) and Li et al. (2016). The data source of basalts from Hawaiian and Azores are as in in Fig. 3.

are uncommon, because the low boron concentrations of these rocks have historically presented challenges to the available methods for high-precision B isotope analysis, i.e., PTIMS via dicesium borate (Nakamura et al., 1992; Tonarini et al., 1997), and/or in-situ ICP-MS analysis (LeRoux et al., 2004). As such, the new B isotopic results presented in this study expand the database for intraplate mantle sources, both in terms of number of measurements and in providing the first high-precision data for rocks derived from subcontinental mantle sources.

Ryan and Chauvel (2014) present a current compilation of available high-precision $\delta^{11}B$ data for mafic volcanic rocks plotted versus Nb/B (after Ishikawa and Nakamura, 1994) as a means of defining the global mixing endmembers for B and B isotopes in relation to subduction processes. We have modified this diagram in Fig. 5 to include our new results and all available high-precision B isotopic data for other ocean ridge and intraplate volcanic settings. The $\delta^{11}B$ signatures of most lavas from modern subduction zones can be explained as a mixture of two B-enriched components, one with very high $\delta^{11}B$ (up to +18‰) and one with much lower $\delta^{11}B$ (as low as −10‰). MORBs and intraplate basalts, including our eastern China suites, record intermediate $\delta^{11}B$ signatures, between −1.4‰ and −7.7‰, at lower boron concentrations than almost any subduction-related lava.

In terms of B concentrations, our data are consistent with the contention (e.g., Ryan et al., 1996) that the mantle sources of intraplate volcanic rocks are relatively poorer in boron than those of ocean ridge or subduction-related
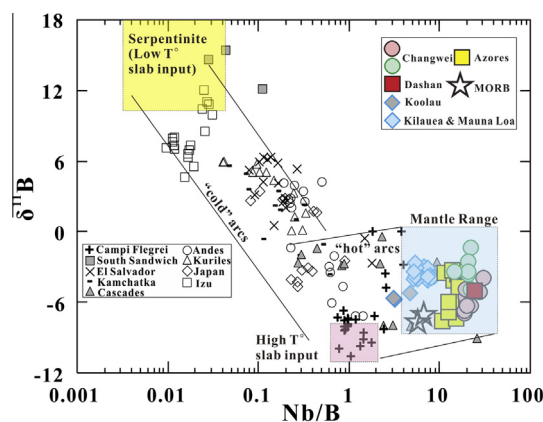


Fig. 5. Diagram of $\delta^{11}B$ versus Nb/B for the global arc basalt database (Ryan and Chauvel, 2014) with data for NCC basalts, other intraplate of Hawaiian from Tanaka and Nakamura (2005) and Tanaka et al. (2002), and Azores of Turner et al. (1997, 2007), and ocean ridge basalts of LeRoux et al. (2004). Our NCC $\delta^{11}B$ suite are consistent with other basalts derived from non-subduction-related mantle sources in that they show and intermediate range of $\delta^{11}B$ values (−1.4‰ to −7.6‰) and very high Nb/B ratios.

lavas, as Nb/B ratios in our eastern NCC basalts range to far higher values than any arc lavas, MORB and most other intraplate lavas, e.g., Hawaiian and Azores basalts (Figs. 4a, 5). The $\delta^{11}B$ of the eastern China basalts argue for an overall intraplate mantle boron isotopic signature of no lower than ∼−7‰, consistent with the results of

Tanaka and Nakamura (2005), Turner et al. (2007) and LeRoux et al. (2004), and similar to the lunar basalt $\delta^{11}B$ signature reported by Zhai et al. (1996). These newer high-precision $\delta^{11}B$ results suggest a heavier B isotopic signature for mantle-derived rocks than was inferred from early ion microprobe analyses (i.e., Chaussidon and Marty, 1995; Roy-Barman et al., 1998), and point out the need for expanding the high-precision B isotope database for fresh mid-ocean ridge and intraplate volcanic samples.

Recent advances in the study of OIBs suggest their sources usually include ancient recycled materials (e.g., Blichert-Toft et al., 1999; Sobolev et al., 2005, 2007; Herzberg, 2011). The B isotope compositions of basalts from Hawaii and the Azores show correlations with their Sr, Nd, and Os isotopic signatures (Tanaka and Nakamura, 2005; Turner et al., 2007) that indicate B isotopes may provide useful information in distinguishing among the mantle sources of OIBs. On a plot of $\varepsilon_{Nd}$ vs $\delta^{11}B$, the Hawaii and Azores samples show a positive correlation with a high $\delta^{11}B$ (about −3‰) high $\varepsilon_{Nd}$ (~6; Fig. 6a) endmember that has higher $\delta^{11}B$ than fresh MORBs



Fig. 6. $\varepsilon_{Nd}$ versus $\delta^{11}B$ (a) and $^{87}Sr/^{86}Sr$ versus $\delta^{11}B$ (b) diagrams for bulk rocks of basalts from western Shandong. The Sr-Nd isotope data of western Shandong basalts are from Zeng et al. (2010) and Li et al. (2016). The data source of Hawaiian and Azores are as in Fig. 3. The MORB (Su and Langmuir, 2003; LeRoux et al., 2004), marine sediments (GLOSS; Plank and Langmuir, 1998; Tonarini et al., 2011) and altered oceanic crust (AOC; Staudigel et al., 1996; Smith et al., 1995; Leeman et al., 2004) values are also plotted in the context. The $\varepsilon_{Nd}$ of the 1.0 Ga AOC (5.4) and GLOSS (−14.1) were calculated after the method of Chauvel et al. (2008).

(LeRoux et al., 2004) but lower values than that of the altered oceanic crust. This higher $\delta^{11}B$ value may reflect the contribution of ancient subducted MORBs, lithospheric mantle or ambient mantle peridotite in the mantle source of OIBs (Tanaka and Nakamura, 2005; Turner et al., 2007). The Hawaiian and Azores samples also share an endmember with low $\delta^{11}B$, low $\varepsilon_{Nd}$ and high $^{87}Sr/^{86}Sr$ (Fig. 6). This endmember is consistent with some role for subducted sediments in their mantle sources. It is thus possible that B isotopic signatures of the OIBs (or at least of Hawaiian and Azores basalts) may thus be governed by varying inputs of subducted sedimentary and ocean crustal materials (Tanaka and Nakamura, 2005; Turner et al., 2007). Our eastern NCC samples show different B-Nd isotope relationships as compared to Hawaii and the Azores, however, indicating that the B isotope characteristics of the mantle beneath the eastern NCC are different from those of intraplate ocean islands.

### 5.3. B isotope heterogeneity in the mantle sources beneath eastern China

Our eastern China data appear to document variation in their B abundance and isotopic signatures that is not related to the effects of differentiation (i.e., not due to crustal assimilation or other possible inputs of exotic [11]B-rich boron). The alkali basalts in our suite are more enriched in Ba, Pb and Sr than the basanites and nephelinites (Fig. 2). However, these rocks do not show significant variation in their B/Nb ratios (Fig. 4a). Divergence between the systematics of B and that of other incompatible elements is also seen among the Hawaiian volcanoes, where the Koolau Makapu'u series lavas (>1 Ma) are similar in $Ce_N/Pb_N$, $Sr/Sr^*$ and $Ba_N/Th_N$ to the more recent Kilauea and Mauna Loa lavas (<0.2 Ma) (Fig. 2b and Supplemental Figures), but have higher B/Nb than either Kilauea or Mauna Loa (Fig. 4a). It would thus appear that the source of the Koolau Makapu'u lavas was enriched in B relative to the sources of more recent Hawaiian lavas, including lavas from Haleakala (Ryan et al., 1996; West and Leeman, 1987), which likely reflect changes in the mantle source contributors to Hawaiian magmatism over time. As such, the observed differences between the systematics of B and other trace elements in the basalts of western Shandong likely reflect differences in mantle sources.

In contrast with published data for the Azores and Hawaii ocean island suites, $\delta^{11}B$ in the western Shandong basalts is negatively correlated with $\varepsilon_{Nd}$ (Fig. 6; Turner et al., 2007; Tanaka and Nakamura, 2005). As boron cannot be isotopically fractionated at magma generation temperatures (Hervig et al., 2002), it is therefore clear that the mantle beneath the eastern NCC is heterogeneous in terms of its boron isotopic signature. The FME-enriched mantle component observed in rocks of the eastern NCC, which is most evident in the signatures of our alkali basalts, has higher $\delta^{11}B$ and lower $\varepsilon_{Nd}$ than the FME-depleted mantle component that is more evident in our NCC basanites and nephelinites (Fig. 6a). Also, there appears to be a clear contribution from a MORB-like source (high $\varepsilon_{Nd}$, low $\delta^{11}B$) in the western Shandong basalts (Fig. 6). The B
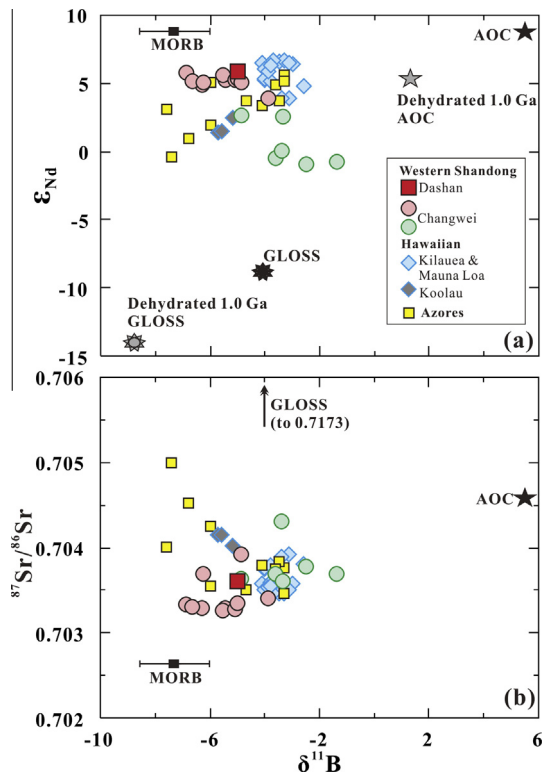
isotopic systematics in western Shandong cannot easily be derived solely via varying material inputs related to an ancient subduction event, as can fresh Hawaiian and Azores basalts. Our alkali basalts have higher $SiO_2$, but lower $FeO^T$ at a given $Mg^\#$, and lower degrees of LREE/HREE fractionation than do our basanites and nephelinites (Supplemental Figures), indicating that the alkali basalt parental magmas were likely derived from shallower mantle depths than basanite or nephelinite parental melts (Li et al., 2014, 2016). It would thus appear that the deeper mantle beneath the eastern NCC has a lower $\delta^{11}B$ than the shallower mantle.

## 5.4. Tectonic implications

### 5.4.1. B isotopes argue against a delamination model for lithospheric thinning

The B isotope systematics of the western Shandong basalts provides new constraints on two aspects of the tectonic evolution of the eastern NCC. The first relates to the mechanism of lithospheric thinning of the eastern NCC. As the high $SiO_2$ basalts of the eastern NCC are FME- (e.g., Ba and Sr) enriched, and are derived from a mantle source affected by materials with an EMI-like isotopic signature (Fig. 2), some workers have argued, based on radiogenic isotopes, that delaminated lower continental crust evolved to become the EMI components in the convective mantle beneath the eastern NCC (e.g., Liu et al., 2008; Chen et al., 2009; Zeng et al., 2011). However, the continental crust preserves a $\delta^{11}B$ value of about −10‰ (Kasemann et al., 2000; van Hinsberg et al., 2011; Marschall and Jiang, 2011). It thus appears that the involvement of this kind of material in the convective mantle is inconsistent with the B isotopic systematics of western Shandong basalts, i.e., the EMI radiogenic isotopic component is associated with higher $\delta^{11}B$ signatures. These higher $\delta^{11}B$ values point to a mantle component that experienced low-temperature (<600 °C) geological processes at or near the earth's surface (Tanaka and Nakamura, 2005). Thus, the B isotope signatures of the western Shandong basalts are more likely related to subduction of oceanic plates rather than delamination of continental crust.

### 5.4.2. Multiple metasomatic events in the mantle beneath the eastern NCC revealed by B isotopes

As discussed above, the petrogenesis of the western Shandong basalts cannot be explained solely via contributions from an ancient subducted component. The wet upwelling model of Kuritani et al. (2011) and Wang et al. (2015) for intracontinental basalt generation in eastern China would constrain the B isotopic signature of western Shandong basalts to be derived from a mixture of materials released from the MTZ (subducted MORB and sedimentary materials). However, the high $\varepsilon_{Nd}$ Shandong samples have low $\delta^{11}B$, unlike what is observed in OIBs (Fig. 6a). As such, a single stage metasomatic event is inadequate to explain the B isotope composition of western Shandong basalts. In order to clarify the contribution of different subducted materials to the mantle's B isotopic heterogeneity, we have conducted Rayleigh fractionation calculations of

the B isotopic compositions for subducted sediments and altered oceanic crust during the progressive dehydration (melting is not taken into account) of a subducted oceanic plate (Table 2). Our calculations indicate that dehydrated oceanic crust (≈+1.3‰) will maintain a higher $\delta^{11}B$ than sediments (≈−8.8‰) even when subducted to 250 km depths.

Based on correlations between B, Nd and Sr isotopes, the alkali basalts reflect the involvement of both subducted altered oceanic crust and marine sediments in their mantle source (Fig. 6), as is also evident based on their Hf-Nd isotope correlations (Li et al., 2014; Supplemental Figures). However, these materials cannot have been derived from the recent subducted Pacific slab (Zeng et al., 2010; Kuritani et al., 2011; Li et al., 2016). Therefore, an ancient subduction event is likely responsible for this mantle reservoir. In view of the differences in mantle isotopic signatures in northern (EMI + DM) and southern (EMII + DM, Fig. 1a) China, this ancient event may be related to a particular geological event in the NCC, i.e., the collision and amalgamation of the eastern and western NCC at ∼1.85 Ga (Zhao et al., 2001). Another possibility is that these materials were transported into the NCC subcontinental mantle via subduction-related mantle convection.

The basanites and nephelinites from this study have lower $\delta^{11}B$ and higher $\varepsilon_{Nd}$ than the alkali basalts (Fig. 6a). These characteristics are broadly similar to available data for St. Helena, though the available B isotope results (early SIMS data: Chaussidon and Marty, 1995; new, high-resolution SIMS: Walowski et al., 2016) make a more detailed comparison difficult. Models for the petrogenesis of the basanites and nephelinites from western Shandong are similar to those that have been proposed for St. Helena basalts, i.e., metasomatism by carbonatite from subducted oceanic crust may be responsible for their HIMU signatures, as well as their low $SiO_2$ high $FeO^T$ and CaO (e.g., Jackson and Dasgupta, 2008). In terms of their major

Table 2

Parameters for calculation of Rayleigh fractionation of B isotope during progressive dehydration.

| | B (μg/g) | $\delta^{11}B$ (‰) | $H_2O$ (wt%) |
|---|---|---|---|
| *Starting composition* | | | |
| Altered oceanic crust | 26 | 5.5 | 7.29 |
| Subducted sediments | 115 | −4.1 | 2.7 |
| *Residual at 250 km depth* | | | |
| Altered oceanic crust | 16.2 | 1.3 | 0.23 |
| Subducted sediments | 74.6 | −8.8 | 0.87 |

B elemental and isotopic data are from Smith et al. (1995), Leeman et al. (2004) and Tonarini et al. (2011), while the initial chemical composition and water content are from Plank and Langmuir (1998) and Staudigel et al. (1996). The dehydration paths are calculated using PerpleX (Connolly, 2005), setting the subduction zone thermal model as that of Bonin arc (Syracuse et al., 2010). The Rayleigh fractionation of B isotope is calculated according the equations of Marschall et al. (2006), partition coefficient of B between hydrous fluids and residual rock of 0.05 (Phengite bearing condication; Marschall et al., 2007), and temperature-dependent B fractionation factor of Hervig et al. (2002).

and trace elements, the nephelinites and basanites from western Shandong have been argued to reflect a mantle source that had experienced metasomatism by carbonatite melts from the subducted Pacific slab (Sakuyama et al., 2013; Li et al., 2016), The most recent B isotope results reported for St. Helena and other HIMU OIBs (i.e., Walowski et al., 2016) appear to be compatible with such a model.

FTIR results for olivines, orthopyroxenes and clinopyroxenes in basalts and peridotite xenoliths reveal that the subcontinental lithospheric mantle beneath the eastern NCC was water rich (>1000 µg/g) at ∼120 Ma (Xia et al., 2013). However, the water contents of the NCC mantle became markedly lower in the Cenozoic ($25 \pm 18$ µg/g; Xia et al., 2010). Thus, a wet upwelling event beneath the NCC is unlikely to relate to the currently subducting Pacific plate, as this subduction began in the Mesozoic (Müller et al., 2008) and lasted to the present (Reagan et al., 2013), during which period the NCC mantle was comparatively dry. It is more likely that the eastern NCC experienced hydration and related metasomatism before subduction of the Pacific plate began (Müller et al., 2008). The contribution of the subducting Pacific slab to mantle heterogeneity beneath the eastern NCC is most likely related to carbonatite and associated silicate melting of carbonated eclogite (Li et al., 2016).

## 6. CONCLUSIONS

Correlations between B and $\delta^{11}$B signatures and other elemental and radiogenic isotopic tracers confirm that the Cenozoic basalts from western Shandong preserve their pre-eruptive B compositions. The B isotopic composition of western Shandong basalts reveal mantle sources that may be vertically heterogeneous. The FME- (e.g., Cs, Ba, K, Pb, and Sr) rich, isotopically EMI-like mantle source within the NCC has higher $\delta^{11}$B than a deeper FME-depleted mantle component that appears to derive from the mantle transition zone. Thus our B isotope results, together with radiogenic Sr-Nd isotopes, suggest the mantle beneath the eastern NCC underwent at least two metasomatic events. The older event created an FME-enriched, higher $\delta^{11}$B mantle source in the convecting mantle above the mantle transition zone, whereas the more recent event (s), related to the ongoing subduction of the Pacific slab, led to the formation of a lower $\delta^{11}$B mantle source at depth.

### ACKNOWLEDGEMENTS

### APPENDIX A. SUPPLEMENTARY DATA

Supplementary data associated with this article can be found, in the online version, at http://dx.doi.org/10.1016/j.gca.2016.08.027.

### REFERENCES

Basu A. R., Junwen W., Wankang H., Guanghong X. and Tatsumoto M. (1991) Major element, REE, and Pb, Nd and Sr isotopic geochemistry of Cenozoic volcanic rocks of eastern China: implications for their origin from suboceanic-type mantle reservoirs. *Earth Planet. Sci. Lett.* **105**, 149–169.

Bercovici D. and Karato S. I. (2003) Whole-mantle convection and the transition-zone water filter. *Nature* **425**, 39–44.

Blichert-Toft J., Frey F. A. and Albarède F. (1999) Hf isotope evidence for pelagic sediments in the source of Hawaiian basalts. *Science* **285**(5429), 879–882.

Brenan J. M., Neroda E., Lundstrom C., Shaw H. F., Ryerson F. J. and Phinney D. L. (1998a) Behavior of boron, beryllium and lithium during melting and crystallization: constraints from mineral-melt partitioning experiments. *Geochim. Cosmochim. Acta* **62**, 2129–2141.

Chaussidon M. and Jambon A. (1994) Boron content and isotopic composition of oceanic basalts: geochemical and cosmochemical implications. *Earth Planet. Sci. Lett.* **121**, 277–291.

Chaussidon M. and Marty B. (1995) Primitive boron isotope composition of the mantle. *Science* **269**, 383–386.

Chauvel C., Lewin E., Carpentier M., Arndt N. T. and Marini J. C. (2008) Role of recycled oceanic basalt and sediment in generating the Hf–Nd mantle array. *Nat. Geosci.* **1**, 64–67.

Chen J. C., Hsu C. N. and Ho K. S. (2003) Geochemistry of Cenozoic volcanic rocks and related ultramafic xenoliths from the Jilin and Heilongjiang provinces, northeast China. *J. Asian Earth Sci.* **21**, 1069–1084.

Chen Y., Zhang Y., Graham D., Su S. and Deng J. (2007) Geochemistry of Cenozoic basalts and mantle xenoliths in northeast China. *Lithos* **96**, 108–126.

Chen L. H., Zeng G., Jiang S. Y., Hofmann A. W., Xu X. S. and Pan M. B. (2009) Sources of Anfengshan basalts: subducted lower crust in the Sulu UHP belt, China. *Earth Planet. Sci. Lett.* **286**, 426–435.

Connolly J. A. D. (2005) Computation of phase equilibria by linear programming: a tool for geodynamic modeling and its application to subduction zone decarbonation. *Earth Planet. Sci. Lett.* **236**, 524–541.

Dasgupta R., Hirschmann M. M. and Smith N. D. (2007) Partial melting experiments of peridotite with $CO_2$ at 3 GPa and genesis of alkalic ocean island basalts. *J. Petrol.* **48**, 2093–2124.

Dasgupta R., Hirschmann M. M., McDonough W. F., Spiegelman M. and Withers A. C. (2009) Trace element partitioning between garnet lherzolite and carbonatite at 6.6 and 8.6 GPa with applications to the geochemistry of the mantle and of mantle-derived melts. *Chem. Geol.* **262**, 57–77.

Faccenna C., Becker T. W., Lallemand S., Lagabrielle Y., Funiciello F. and Piromallo C. (2010) Subduction-triggered magmatic pulses: a new class of plumes? *Earth Planet. Sci. Lett.* **299**, 54–68.

Fan Q. C. and Hooper P. R. (1991) The Cenozoic basaltic rocks of eastern China: petrology and chemical composition. *J. Petrol.* **32**, 765–810.

Fan W. M. and Menzies M. A. (1992) Destruction of aged lower lithosphere and accretion of asthenosphere mantle beneath eastern China. *Geotectonica et Metallogenia* **16**, 171–180.

Feigenson M. D., Hofmann A. W. and Spera F. J. (1983) Case srudies on the origin of basalt II. The transition from tholeiitic to alkali volcanism on Kohala volcano, Hawaii. *Contrib. Mineral. Petrol.* **84**, 309–405.

Fukao Y., Obayashi M., Inoue H. and Nenbai M. (1992) Subducting slab stagnant in the mantle transition zone. *J. Geophys. Res.* **97**, 4809–4822.

Gao S., Rudnick R. L., Yuan H. L., Liu X. M., Liu Y. S., Xu W. L., Ling W. L., Ayers J., Wang X. C. and Wang Q. H. (2004) Recycling lower continental crust in the North China craton. *Nature* **432**, 892–897.

Genske F. S., Turner S. P., Beier C., Chu M. F., Tonarini S., Pearson N. J. and Haase K. M. (2014) Lithium and boron isotope systematics in lavas from the Azores islands reveal crustal assimilation. *Chem. Geol.* **373**, 27–36.

Griffin, W. L., O'Reilly, S. Y. and Ryan, C. G. (1992) Composition and thermal structure of the lithosphere beneath South Africa, Siberia and China: porton microprobe studies. Abstract of the International Symposium on Cenozoic Volcanic Rocks and Deep-seated Xenoliths of China and its Environs. Beijing, pp. 65–66.

Griffin W. L., Zhang A. D., O'Reilly S. Y. and Ryan C. G. (1998) Phanerozoic evolution of the lithosphere beneath the Sino-Korean craton. In *Mantle Dynamics and Plate Interactions in East Asia*, 27 (eds. M. F. J. Flower, S. L. Chung, C. H. Lo and T. Y. Lee), pp. 107–126. Geodynamics Series. AGU, Washington, D. C.

Guo P. Y., Niu Y. L., Sun P., Ye L., Liu J. J., Zhang Y., Feng Y. X. and Zhao J. X. (2016) The origin of Cenozoic basalts from central Inner Mongolia, East China: the consequence of recent mantle metasomatism genetically associated with seismically observed paleo-Pacific slab in themantle transition zone. *Lithos* **240–243**, 104–118.

Hervig R. L., Moore G. M., Williams L. B., Peacock S. M., Holloway J. R. and Roggensack K. (2002) Isotopic and elemental partitioning of boron between hydrous fluid and silicate melt. *Am. Mineral.* **87**, 769–774.

Herzberg C. (2011) Identification of source lithology in the Hawaiian and Canary Islands: implications for origins. *J. Petrol.* **52**, 113–146.

Hsu C.-N., Chen J.-C. and Ho K.-S. (2000) Geochemistry of Cenozoic volcanic rocks from Kirin Province, northeast China. *Geochem. J.* **34**, 33–58.

Huang J. L. and Zhao D. P. (2006) High-resolution mantle tomography of China and surrounding regions. *J. Geophys. Res.* **111**, B09305. http://dx.doi.org/10.1029/2005JB004066.

Huang X., Xu Y. and Karato S. I. (2005) Water content in the transition zone from electrical conductivity of wadsleyite and ringwoodite. *Nature* **434**, 746–749.

Ishikawa T. and Nakamura E. (1992) Boron isotope geochemistry of the oceanic crust from DSDP/ODP hole 504B. *Geochim. Cosmochim. Acta* **56**, 1633–1639.

Ishikawa T. and Nakamura E. (1994) Origin of the slab component in arc lavas from across-arc variation of B and Pb isotopes. *Nature* **370**, 205–208.

Jackson M. G. and Dasgupta R. (2008) Compositions of HIMU, EM1, and EM2 from global trends between radiogenic isotopes and major elements in ocean island basalts. *Earth Planet. Sci. Lett.* **276**(1–2), 175–186.

Kasemann S., Erzinger J. and Franz G. (2000) Boron cycling in the continental crust of the central Andes from the Paleozoic to Mesozoic, NW Argentina. *Contrib. Miner. Petrol.* **140**, 328–343.

Kısakűrek B., James R. H. and Harris N. B. W. (2005) Li and δ7Li in Himalayan rivers: proxies for silicate weathering? *Earth Planet. Sci. Lett.* **237**, 387–401.

Kuritani T. and Nakamura E. (2006) Elemental fractionation in lavas during post-eruptive degassing: evidence from trachytic lavas, Rishiri Volcano, Japan. *J. Volcanol. Geoth. Res.* **149**, 124–138.

Kuritani T., Kimura J. I., Miyamoto T., Wei H. Q., Shimano T., Maeno F., Jin X. and Taniguchi H. (2009) Intraplate magmatism related to deceleration of upwelling asthenospheric mantle: implications from the Changbaishan shield basalts, northeast China. *Lithos* **112**, 247–258.

Kuritani T., Ohtani E. and Kimura J.-I. (2011) Intensive hydration of the mantle transition zone beneath China caused by slab stagnation. *Nat. Geosci.* **4**, 713–716.

Leeman W. P., Tonarini S., Chan L. H. and Borg L. E. (2004) Boron and lithium isotope variations in a hot subduction zone — the southern Washington Cascades. *Chem. Geol.* **212**, 101–124.

LeRoux P. J., Shirey S. B., Benton L., Hauri E. H. and Mock T. D. (2004) In situ, multiple-multiplier, laser ablation ICP-MS measurement of boron isotopic composition (δ11B) at the nanogram level. *Chem. Geol.* **203**, 123–138.

Li H. Y., Huang X. L. and Guo H. (2014) Geochemistry of Cenozoic basalts from the Bohai Bay Basin: implications for a heterogeneous mantle source and lithospheric evolution beneath the eastern North China Craton. *Lithos* **196–197**, 54–66.

Li H. Y., Xu Y. G., Ryan J. G., Huang X. L., Ren Z. Y., Guo H. and Ning Z. G. (2016) Olivine and melt inclusion chemical constraints on the source of intracontinental basalts from the eastern North China Craton: discrimination of contributions from the subducted Pacific slab. *Geochim. Cosmochim. Acta* **178**, 1–19.

Liu D. Y., Nutman A. P., Compston W., Wu J. S. and Shen Q. H. (1992) Remnants of ≥3800 Ma crust in the Chinese part of the Sino-Korean Craton. *Geology* **20**, 339–342.

Liu C. Q., Masuda A. and Xie G. H. (1994) Major- and trace-element compositions of Cenozoic basalts in eastern China: petrogenesis and mantle source. *Chem. Geol.* **114**, 19–42.

Liu Y. S., Gao S., Kelemen P. B. and Xu W. L. (2008) Recycled crust controls contrasting source compositions of Mesozoic and Cenozoic basalts in the North China Craton. *Geochim. Cosmochim. Acta* **72**, 2349–2376.

Liu J., Xia Q. K., Deloule E., Chen H. and Feng M. (2015) Recycled oceanic crust and marine sediment in the source of alkali basalts in Shandong, eastern China: evidence from magma water content and oxygen isotopes. *J. Geophys. Res. Solid Earth* **120**. http://dx.doi.org/10.1002/2015JB012476.

Marschall H. R. and Jiang S. Y. (2011) Tourmaline isotopes: no element left behind. *Elements* **7**, 313–319.

Marschall H. R., Ludwig T., Altherr R., Kalt A. and Tonarini S. (2006) Syros metasomatic tourmaline: evidence for very high-δ11B fluids in subduction zone. *J. Petrol.* **47**, 1915–1942.

Marschall H. R., Altherr R. and Rüpke L. (2007) Squeezing out the slab — modelling the release of Li, Be and B during progressive high-pressure metamorphism. *Chem. Geol.* **239**, 323–335.

McDonough W. F. and Sun S. S. (1995) The composition of the Earth. *Chem. Geol.* **120**, 223–253.

Menzies M. A., Fan W. M. and Zhang M. (1993) Palaeozoic and Cenozoic lithoprobe and the loss of >120 km of Archean lithosphere, Sino-Korean craton, China. In *Magmatic Processes and Plate Tectonic*, 76 (eds. H. M. Prichard, T. Alabaster, N. B. W. Harris and C. R. Neary), pp. 71–81. Magmatic Processes and Plate Tectonic. Geological Society, Special Publication.

Morgan W. J. (1971) Convection plumes in the lower mantle. *Nature* **230**, 42–43.

Müller R. D., Sdrolias M., Gaina C., Steinberger B. and Heine C. (2008) Long-term sea-level fluctuations driven by ocean basin dynamics. *Science* **319**, 1357–1362.

Murphy D. T., Kamber B. S. and Collerson K. D. (2003) A refined solution to the first terrestrial Pb-isotope paradox. *J. Petrol.* **44**, 39–53.

Nakamura E., Ishikawa T., Birck J.-L. and Allègre C. J. (1992) Precise boron isotopic analysis of natural rock samples using a boron-mannitol complex. *Chem. Geol.* **94**(3), 193–204.

Pearce J. A., Kempton P. D. and Gill J. B. (2007) Hf–Nd evidence for the origin and distribution of mantle domains in the SW Pacific. *Earth Planet. Sci. Lett.* **260**, 98–114.

Pearson D. G., Brenker F. E., Nestola F., McNeill J., Nasdala L., Hutchison M. T., Matveev S., Mather K., Silversmit G., Schmitz S., Vekemans B. and Vincze L. (2014) Hydrous mantle transition zone indicated by ringwoodite included within diamond. *Nature* **507**, 221–224.

Plank T. and Langmuir C. H. (1998) The chemical composition of subducting sediment and its consequences for the crust and mantle. *Chem. Geol.* **145**, 325–394.

Reagan M. K., McClelland W. C., Girard G., Goff K. R., Peate D. W., Ohara Y. and Stern R. J. (2013) The geology of the southern Mariana fore-arcc rust: implications for the scale of Eocene volcanism in the western Pacific. *Earth Planet. Sci. Lett.* **380**, 41–51.

Rehkämper M. and Hofmann A. W. (1997) Recycled ocean crust and sediment in Indian Ocean MORB. *Earth Planet. Sci. Lett.* **147**, 93–106.

Roy-Barman M., Wasserburg G. J., Pappanastasiou D. A. and Chaussidon M. (1998) Osmium isotopic compositions and Re–Os concentrations in sulfide globules from basaltic glasses. *Earth Planet. Sci. Lett.* **154**, 331–347.

Rudnick R. L. and Gao S. (2003) Composition of the continental crust. In *Treatise on Geochemistry* (ed. R. L. Rudnick). Elsevier, pp. 1–64.

Ryan J. G. and Chauvel C. (2014) The subduction-zone filter and the impact of recycled materials on the evolution of the mantle. In *Treatise on Geochemistry*, vol. 3 (eds. H. D. Holland and K. K. Turekian). Elsevier, Oxford, pp. 479–508, 2nd ed.

Ryan J. G., Leeman W. P., Morris J. D. and Langmuir C. H. (1996) The boron systematics of intraplate lavlas: implications for crust and mantle evolution. *Geochim. Cosmochim. Acta* **60**, 415–422.

Sakuyama T., Tian W., Kimura J.-I., Fukao Y., Hirahara Y., Takahashi T., Senda R., Chang Q., Miyazaki T., Obayashi M., Kawabata H. and Tatsumi Y. (2013) Melting of dehydrated oceanic crust from the stagnant slab and of the hydrated mantle transition zone: constraints from Cenozoic alkaline basalts in eastern China. *Chem. Geol.* **359**, 32–48.

Schmandt B., Jacobsen S. D., Becker T. W., Liu Z. and Dueker K. G. (2014) Dehydration melting at the top of the lower mantle. *Science* **344**, 1265–1268.

Sleep N. H. and Zahnle K. (2001) Carbon dioxide cycling and implications for climate on ancient Earth. *J. Geophys. Res.* **106**, 1373–1399.

Smith H. J., Spivack A. J., Staudigel H. and Hart S. R. (1995) The boron isotopic composition of altered oceanic crust. *Chem. Geol.* **126**, 119–135.

Sobolev A. V., Hofmann A. W., Sobolev S. V. and Nikogosian I. K. (2005) An olivine-free mantle source of Hawaiian shield basalts. *Nature* **434**, 590–597.

Sobolev A. V., Hofmann A. W., Kuzmin D. V., Yaxley G. M., Arndt N. T., Chung S. L., Danyushevsky L. V., Elliott T., Frey F. A., Garcia M. O., Gurenko A. A., Kamenetsky V. S., Kerr A. C., Krivolutskaya N. A., Matvienkov V. V., Nikogosian I.

K., Rocholl A., Sigurdsson I. A., Sushchevskaya N. M. and Teklay M. (2007) The amount of recycled crust in source of mantle-derived melts. *Nature* **316**, 412–417.

Spivack A. J. and Edmond J. M. (1987) Boron isotopic exchange between seawater and the oceanic crust. *Geochim. Cosmochim. Acta* **51**, 1033–1043.

Staudigel, H., Plank, T., White, W.M. and Schmincke, H. (1996) Geochemical fluxes during seafloor alteration of the upper oceanic crust: DSDP Sites 417 and 418. In: *Subduction Top to Bottom: AGU Monograph* (eds. G. E. Bebout, D. Scholl, S. Kirby and J. P. Platt), 96, pp. I19–I38.

Su, Y. and Langmuir, C. H. (2003) Global MORB chemistry compilation at the segment scale. PhD thesis, Department of Earth and Environmental Sciences, Columbia University. Available at: http://petdb.ldeo.columbia.edu/documentation/morbcompilation/.

Sun S. S. and McDonough W. F. (1989) Chemical and isotopic systematics of oceanic basalts: implications for mantle composition and processes. In *Magmatism in the Ocean Basins*, 42 (eds. A. D. Saunders and M. J. Norry). Geological Society Special Publication, London, pp. 313–345.

Syracuse E. M., Van Keken P. E. and Abers G. A. (2010) The global range of subduction zone thermal models. *Phys. Earth Planet. Inter.* **183**, 73–90.

Tanaka R. and Nakamura E. (2005) Boron isotopic constraints on the source of Hawaiian shield lavas. *Geochim. Cosmochim. Acta* **69**(13), 3385–3399.

Tanaka, R., Nakamura, E. and Takahashi, E. (2002) Geochemical evolution of Koolau volcano. In *Hawaiian Volcanoes: Deep Underwater Perspectives*, Vol. 128 (eds. E. Takahashi, P. W. Lipman, M. O. Garcia, J. Naka and S. Aramaki), pp. 311–332. AGU Geophysical Monograph.

Tang Y. C., Obayashi M., Niu F. L., Grand S. P., Chen Y. J., Kawakatsu H., Tanaka S., Ning J. Y. and Ni J. F. (2014) Changbaishan volcanism in northeast China linked to subduction-induced mantle upwelling. *Nat. Geosci.* **7**, 470–474.

Thomson A. R., Walter M. J., Kohn S. C. and Brooker R. A. (2016) Slab melting as a barrier to deep carbon subduction. *Nature* **529**, 76–79.

Tonarini S., Pennisi M. and Leeman W. (1997) Precise boron isotopic analysis of complex silicate (rock) samples using alkali carbonate fusion and ion-exchange separation. *Chem. Geol.* **142** (1–2), 129–137.

Tonarini S., Leeman W. P. and Leat P. L. (2011) Subduction erosion of forearc mantle wedge implicated in the genesis of the South Sandwich Island (SSI) arc: evidence from boron isotope systematics. *Earth Planet. Sci. Lett.* **301**, 275–284.

Turner S., Hawkesworth C., Rogers N. and King P. (1997) U-Th isotope disequilibria and ocean island basalt generation in the Azores. *Chem. Geol.* **139**, 145–164.

Turner S., Tonarini S., Bindeman L., Leeman W. P. and Schaefer B. F. (2007) Boron and oxygen isotope evidence for recycling of subducted components over the past 2.5 Gyr. *Nature* **447**, 702–705.

van Hinsberg V. J., Henry D. J. and Marschall H. R. (2011) Tourmaline: an ideal indicator of its host environment. *Can. Mineral.* **49**, 1–16.

Walowski, K., Kirstein, L., Jan de Hoog C., Elliot T., Savov I., and Devey, C. (2016) Tracing recycled volatiles in a heterogeneous mantle with boron isotopes. Geophysical Research Abstracts, Vol. 18, EGU2016-15761, EGU General Assembly 2016.

Wang X. C., Wilde S. A., Li Q. L. and Yang Y. N. (2015) Continental flood basalts derived from the hydrous mantle transition zone. *Nat. Commun.* **6**. http://dx.doi.org/10.1038/ncomms8700 7700.

Wei G. J., Wei J. X., Liu Y., Ke T., Ren Z. Y., Ma J. L. and Xu Y. G. (2013) Measurement on high-precision boron isotope of silicate materials by a single column purification method and MC-ICP-MS. *J. Anal. At. Spectrom.* **28**, 606–612.

West H. B. and Leeman W. P. (1987) Isotopic evolution of lavas from Haleakala Crater, Hawaii. *Earth Planet. Sci. Lett.* **84**(2–3), 211–225.

Willbold M. and Stracke A. (2006) Trace element composition of mantle end-members: implications for recycling of oceanic and upper and lower continental crust. *Geochem. Geophys. Geosyst.* **7**. http://dx.doi.org/10.1029/2005gc001005.

Workman R. K. and Hart S. R. (2005) Major and trace element composition of the depleted MORB mantle (DMM). *Earth Planet. Sci. Lett.* **231**, 53–72.

Wu F. Y., Lin J. Q., Wilde S. A., Zhao X. O. and Yang J. H. (2005) Nature and significance of the early Cretaceous giant igneous event in Eastern China. *Earth Planet. Sci. Lett.* **233**, 103–119.

Xia Q. K., Hao Y. T., Li P., Deloule E., Coltorti M., Dallai L., Yang X. Z. and Feng M. (2010) Low water content of the Cenozoic lithospheric mantle beneath the eastern part of the North China Craton. *J. Geophys. Res.* **115**, B07207.

Xia Q. K., Liu J., Liu S. C., Kovács I., Feng M. and Dang L. (2013) High water content in Mesozoic primitive basalts of the North China Craton and implications for the destruction of cratonic mantle lithosphere. *Earth Planet. Sci. Lett.* **361**, 85–97.

Xu Y. G. (2001) Thermo-tectonic destruction of the Archean lithospheric keel beneath eastern China: evidence, timing and mechanism. *Phys. Chem. Earth (A)* **26**, 747–757.

Xu Y. G., Chung S. L., Ma J. L. and Shi L. B. (2004) Contrasting Cenozoic lithospheric evolution and architecture in the Western and Eastern Sino-Korean Craton: constraints from geochemistry of basalts and mantle xenoliths. *J. Geol.* **112**, 593–605.

Xu Y. G., Zhang H. H., Qiu H. N., Ge W. C. and Wu F. Y. (2012a) Oceanic crust components in continental basalts from Shuangliao, Northeast China: derived from the mantle transition zone? *Chem. Geol.* **328**, 168–184.

Xu Z., Zhao Z. F. and Zheng Y. F. (2012b) Slab–mantle interaction for thinning of cratonic lithospheric mantle in North China: geochemical evidence from Cenozoic continental basalts in central Shandong. *Lithos* **146**, 202–217.

Yan J. and Zhao J. X. (2008) Cenozoic alkali basalts from Jingpohu, NE China: the role of lithosphere–asthenosphere interaction. *J. Asian Earth Sci.* **33**, 106–121.

Zeng G., Chen L. H., Xu X. S., Jiang S. Y. and Hofmann A. W. (2010) Carbonated mantle sources for Cenozoic intra–plate alkaline basalts in Shandong, North China. *Chem. Geol.* **273**, 35–45.

Zeng G., Chen L. H., Hofmann A. W. and Xu X. S. (2011) Crust recycling in the sources of two parallel volcanic chains in Shandong, North China. *Earth Planet. Sci. Lett.* **302**, 359–368.

Zhai M., Nakamura E., Shaw D. M. and Nakano T. (1996) Boron isotope ratios in meteorites and lunar rocks. *Geochim. Cosmochim. Acta* **60**(23), 4877–4881.

Zhao D. P. (2004) Global tomographic images of mantle plumes and subducting slabs: insight into deep Earth dynamics. *Phys. Earth Planet. Inter.* **146**, 3–34.

Zhao G. C., Wilde S. A., Cawood P. A. and Sun M. (2001) Archean blocks and their boundaries in the North China Craton: lithological, geochemical, structural and P-T path constraints. *Precambr. Res.* **107**, 45–73.

Zhao D. P., Tian Y., Lei J. S., Liu L. C. and Zheng S. H. (2009) Seismic image and origin of the Changbai intraplate volcano in East Asia: role of big mantle wedge above the stagnant Pacific slab. *Phys. Earth Planet. Inter.* **173**, 197–206.

Zheng J. P., O'Reilly S. Y., Griffin W. L., Lu F. X. and Zhang M. (1998) Nature and evolution of cenozoic lithospheric mantle beneath Shandong Peninsula North China platform. *Int. Geol. Rev.* **40**, 471–499.

Zhou X. H. and Armstrong R. L. (1982) Cenozoic volcanic rocks of eastern China—secular and geographic trends in chemistry and strontium isotopic composition. *Earth Planet. Sci. Lett.* **59**, 301–329.

Zindler A. and Hart S. (1986) Chemical geodynamics. *Annu. Rev. Earth Planet. Sci.* **14**, 493–571.

Zou H., Fan Q. and Yao Y. (2008) U-Th systematic of dispersed young volcanoes in NE China: asthenosphere upwelling caused by pilling up and upward thickening of stagnant Pacific slab. *Chem. Geol.* **255**, 134–142.

*Associate editor:* Horst Marschall